Transport investigations in pellet-fuelled plasmas of ASDEX Upgrade

F. Gschoesser, C. Angioni, P. T. Lang, M. Bergmann, E. Fable, R. Fischer, B. Ploeckl, F. Stefanelli, D. Stieglitz, G. Tardini, H. Zohm and the ASDEX Upgrade Team*
Max-Planck-Institute for Plasma Physics, Garching, Germany

florian.gschoesser@ipp.mpg.de

1 Introduction

Pellet injection is currently regarded as the most promising way to efficiently fuel reactor-relevant plasmas. However, the pellet can have a substantial perturbative effect on the background plasma. To develop an optimized pellet fueling system, it is important to obtain a better understanding of the physics of the pellet-plasma interaction. The goal of this work is to model these processes by simulation with SMART [1], ASTRA [2], and TGLF-SAT2 [3] and to compare to the experimental results of the tokamak ASDEX Upgrade, both in H-mode and L-mode cases.

2 The ASDEX Upgrade pellet launching system

For a detailed description see [4] and [5]. To gain knowledge of in what condition the pellets arrive at the plasma, one has to have a basic understanding of the creation of the pellets themselves. The ASDEX Upgrade pellet launching system comprises the following key parts: **Pellet source:** Hydrogen (mostly deuterium) is resublimated at around 10K, compressed, and extruded into a 19cm long rod. This cubical rod has a nominal cross section of $1.9 \times 1.9\text{mm}^2$ in the case of large pellets; **Storage cryostat:** This rod is stored and cooled until pellets are requested in the experiment. On request, the rod is cut into 2mm long (in the case of large) pellets, which drop into the **Centrifuge** for acceleration, in this case to 240m/s. **Guiding tube:** The accelerated pellets are then guided through a tube ("looping") towards the high-field side (HFS) injection port, where they enter the plasma vessel.

During this whole process, the pellets lose a part of their mass. This mass loss seems to be highly variable and can have a large spread of up to approximately 50%. Some pellets also break into parts, and others get lost completely. In this work, for comparison to the experiment, in the simulations we introduce a free parameter, the so-called "pellet efficiency", an adjustment of the total amount of particles a pellet contains. This adjustment is aiming for a small correction; if the pellet size varied too much, they were excluded from the evaluation.

3 The pellet-plasma interaction

The interaction of the pellet with the background plasma can be divided into three phases, which overlap:

- Pellet Ablation ($t < 2$ms): Pellet material ablates and forms a gas cloud around the pellet. Excitation and recombination effects result in light emission.
- Pellet Particle Deposition ($t \approx 2$ms): The grad-B drift combined with a non-axisymmetric density perturbation induces a drift of the ionized pellet-material towards the low-field side (LFS). High-field side (HFS) injection, as a result, leads to a much deeper particle deposition.
- Transport ($t \approx 50$ms): Large modifications of the plasma profiles (after the pellet material got ionized and distributed along the flux surfaces) lead to additional transport effects.

4 Improvement of the signal-to-noise ratio

As the pellet perturbation occurs on short time scales (in the order of a few milliseconds), it is difficult to find diagnostics with both a high time resolution and a good signal-to-noise ratio (SNR). To address this, a dedicated shot has been designed to mitigate these problems using a statistical approach, namely

*See author list of T. Pütterich et al 2026 Nucl. Fusion, 66, 116002 averaging over multiple similar pellets. The assumption is that pellets are independent from each other, meaning that after each pellet perturbation enough time has passed to relax all profiles. As shown in figure 1a, this assumption has been fulfilled at least approximately for the shot AUG #43337, the H-mode reference scenario in this work, with the following main discharge parameters (before the pellet): $I_p = 800\text{kA}$, $B_t = 2.6\text{T}$, $q_{95} = 5.4$, $P_{NBI} = 9.8\text{MW}$, $P_{ICRH} = 1.62\text{MW}$, $n_{e,core} \approx 9.5 \cdot 10^{19}\text{m}^{-3}$.

Figures 1b and 1c show the improved SNR of the line-integrated density perturbation, averaged over multiple pellets. This lead to a good fit of the stretched exponential decay function ($\propto \exp{(t/\tau)^{\alpha}}$), that describes the data well. For the L-mode scenario, AUG #43895, the same assumption could not be made, but due to much better diagnostics in the new campaign (mostly an improved Thomson scattering diagnostics), the results are still very comparable. Discharge parameters are (before the pellet): $I_p = 800\text{kA}$, $B_t = 2.5\text{T}$, $q_{95} = 5.25$, $P_{NBI} = 0.85\text{MW}$, $n_{e,core} \approx 5.6 \cdot 10^{19}\text{m}^{-3}$.

Figure 2 shows the depositon profile and its time evolution for both L- and H-mode, measured with Thomson scattering, where the H-mode measurements have been improved with the above described technique.

Important to note are three points: First, the pellet penetration is much deeper in the L-mode (maximum at around $\rho_{tor} \approx 0.4$), than in the H-mode ($\rho_{tor} \approx 0.7$). Second, since the injected pellets are similar in size, and therefore have same number of particles, the local density perturbation is roughly double compared to the H-mode (the volume of the flux surface decreases with smaller ρ_{tor}). Third, probably due to much higher relative perturbation and the deeper penetration, the density peak decays much slower in the L-mode.

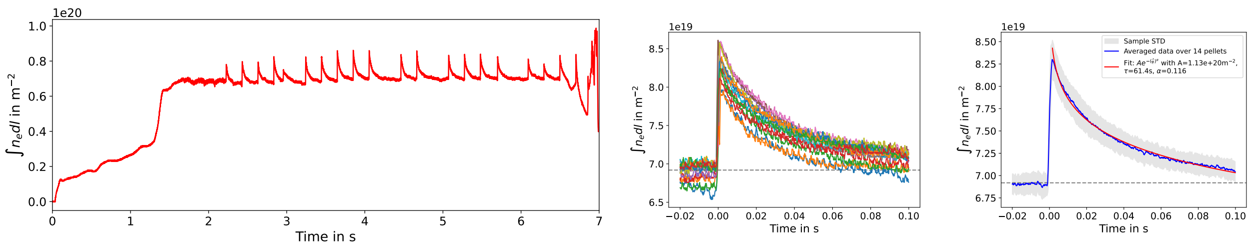

(a) (b) (c)

Figure 1: Line-integrated density of experiment AUG #43337. Plot (a) shows the time evolution of multiple pellets. Similar pellets (b) are being averaged over to get a good signal with little noise, where it turned out that a stretched exponential fits the data well (c).

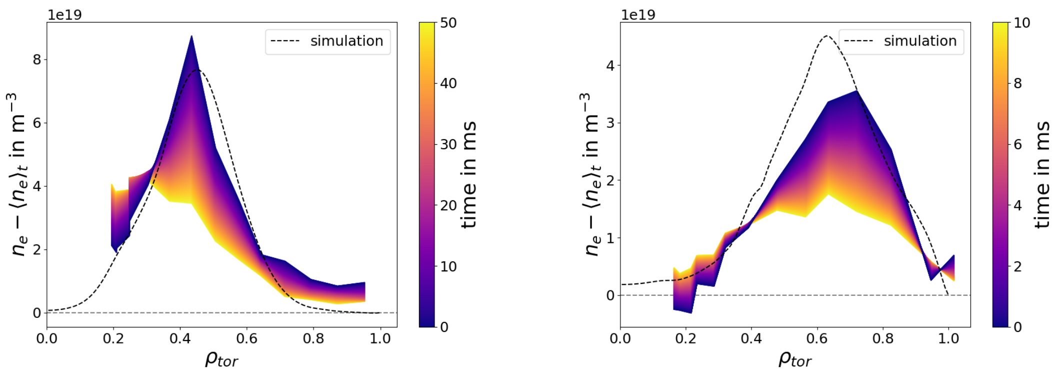

(a) L-mode (b) H-mode

Figure 2: Deposition profiles and their time evolution for L-mode (a) and H-mode (b), measured with Thomson scattering. The black dotted line represents the deposition profile used in the simulations: (a) A Gaussian centered around $\rho_{tor} = 0.4$; (b) The profile computed by SMART. Note the different time scales between L-mode and H-mode.

5 Comparison of simulations to the experiment

For the L-mode, full-radius simulations with the 1D transport code ASTRA [2], combined with the quasilinear turbulent transport solver TGLF-SAT2 [3] were compared to the experiment AUG #43895. The pellet ablation and deposition code SMART [1] could not provide a reasonable retrodiction for the pellet deposition. Therefore, a Gaussian source term, mimicking the pellet injection was used. Its free parameters are based on Thomson scattering measurements (figure 2a).

For the H-mode case, full-radius simulations with ASTRA + TGLF-SAT2 were compared to the experiment AUG #43337. SMART provided a very reasonable pellet deposition profile that could be used as an input for ASTRA (see figure 2b). Also, the simulations included a pedestal pressure feedback loop to accurately capture the H-mode pedestal. Figures 3 and 4 show the comparison of L-mode and H-mode for the electron density.

The overall agreement to the experiment is good in both cases (see figure 5). Especially in the L-mode, the temperature perturbation and its recovery after a pellet injection is reproduced well. The L-mode density increases slightly slower in the core and decays slower at around midradius ($\rho_{tor} = 0.51$, figure 5a). This suggests that the particle transport both inwards and outwards is being underpredicted. This result is also robust against a small change of parameters of the Gaussian pellet source. A similar picture emerges for the H-mode density: There is a small overshoot in the core temperature that is not seen in the experiment; with this exception that still has to be clarified, the H-mode temperature evolution is also in very good agreement with the experiment. The inital density decay at mid-radius is slightly slower than in the experiment; this is compensated however rather quickly due to the faster time scales of the H-mode case.

It is important to note that the values for density and temperature are almost halved in the L-mode plasma. Nonetheless, the investigated L-mode case has a much longer pellet particle decay time than the H-mode. A deeper penetration of the pellet into the plasma could at least partially explain this observation. It also takes much longer to recover the temperature drop induced by the pellet, which is related to the lower heating power, and also the larger relative drop of temperature, since the density is lower, but the pellets have the same size.

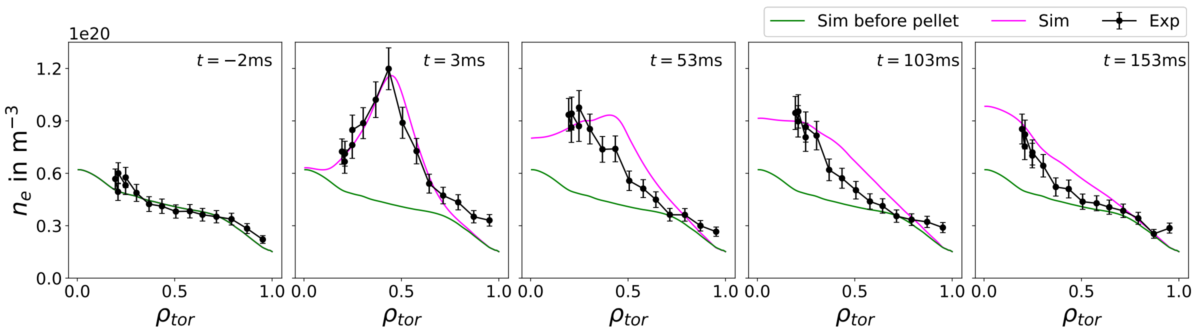

Figure 3: L-mode: Comparison of measured Thomson scattering density profiles with the ASTRA simulation.

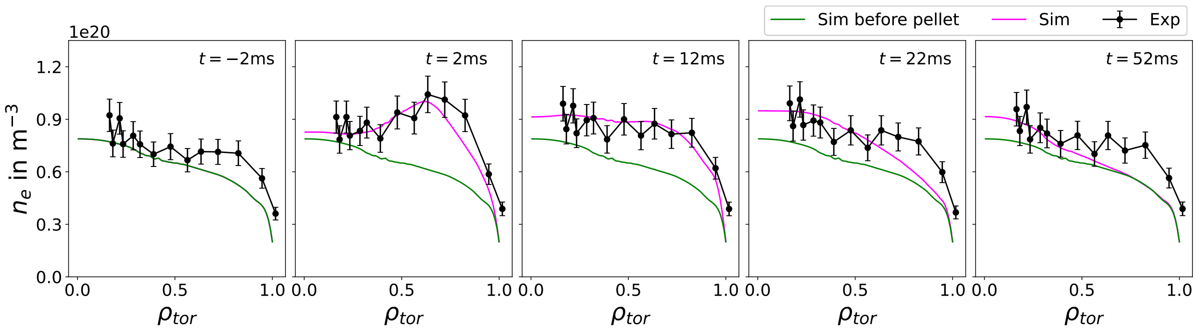

Figure 4: H-mode: Comparison of measured Thomson scattering density profiles with the ASTRA simulation.

6 Conclusions and Outlook

Dedicated experiments with pellets injections were conducted. Experimental data could be improved by taking a statistical approach using the average over multiple similar pellet perturbations. Based on these data, ASTRA[2] simulations with the TGLF-SAT2[3] transport model have been performed. This allowed the retrodiction of the entire time evolution of the plasma response after a pellet injection for a direct comparison with the time evolution of the measured plasma profiles. The SMART[1] code computes pellet ablation and deposition in H-mode very well, but could not be applied for the L-mode. For both H- and L-mode, the simulation retrodicts the temperature recovery after a pellet very well (with an overshoot of the core temperature), but underpredicts particle transport, both inwards and outwards (especially in L-mode). Due to the direct comparison, it could be shown that the pellet particle confinement times in the investigated L-mode case are significantly longer than in the H-mode case. This is largely due to the deeper

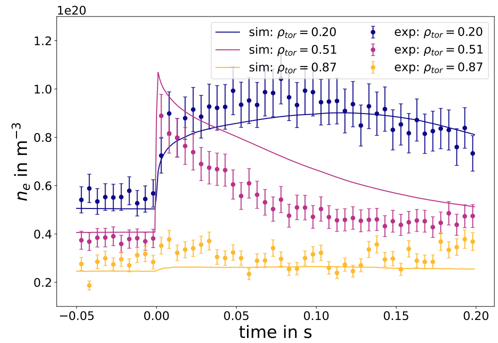

(a) L-mode density

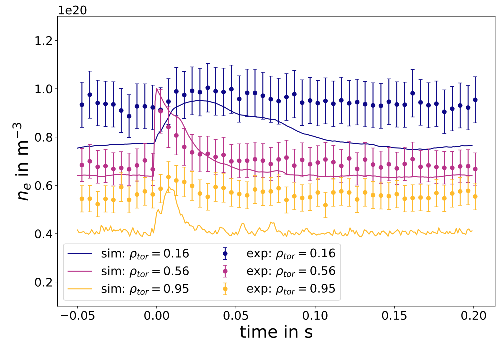

(b) H-mode density

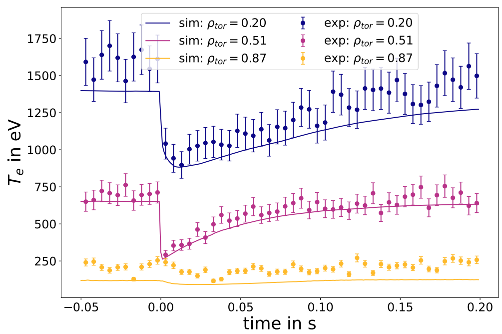

(c) L-mode temperature

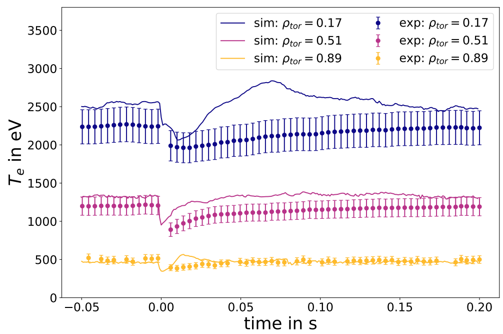

(d) H-mode temperature

Figure 5: Time evolution of different radial points for L-mode (left), H-mode (right), electron density (upper) and electron temperature (lower).

pellet penetration depth in the L-mode case, while the pellet size remains the same.
In the experiment, when pellets are injected at high frequency, one observes a drop in the stored energy W_{MHD}. The reason for this is rather unclear and could be connected to a combination of pedestal and core effects. Reproducing and understanding this behavior is an additional goal of the present activity dedicated to the characterization and the modelling of plasmas with pellet injections.

Acknowledgements

This work has been carried out within the framework of the EUROfusion Consortium, funded by the European Union via the Euratom Research and Training Programme (Grant Agreement No 101052200 — EUROfusion). Views and opinions expressed are however those of the author(s) only and do not necessarily reflect those of the European Union or the European Commission. Neither the European Union nor the European Commission can be held responsible for them.

References

[1] AR Polevoi and M Shimada. Simplified mass ablation and relocation treatment for pellet injection optimization. *Plasma Physics and Controlled Fusion*, 43(11):1525–1533, 2001.

[2] G Tardini, E Fable, C Angioni, M Bergmann, D Fajardo, and T Luda. ASTRA-8: a modern framework for transport analysis and modelling in fusion devices. *Plasma Physics and Controlled Fusion*, 68(6):065024, jun 2026.

[3] Gary M Staebler, EA Belli, J Candy, JE Kinsey, H Dudding, and B Patel. Verification of a quasi-linear model for gyrokinetic turbulent transport. *Nuclear Fusion*, 61(11):116007, 2021.

[4] B Ploeckl and PT Lang. The enhanced ASDEX Upgrade pellet centrifuge launcher. *Review of Scientific Instruments*, 84(10):103509, 2013.

[5] B Ploeckl et al. Advanced ASDEX Upgrade pellet guiding system design. *Review of Scientific Instruments*, 91(8):083502, 08 2020.